A Photolabile Oligodeoxyribonucleotide Probe of the Decoding Site in the Small Subunit of the *Escherichia coli* Ribosome: Identification of Neighboring Ribosomal Components†

Parimi Muralikrishna and Barry S. Cooperman*

Department of Chemistry, University of Pennsylvania, Philadelphia, Pennsylvania 19104-6323

Received October 5, 1993; Revised Manuscript Received November 24, 1993®

ABSTRACT: In this work we report the synthesis of a radioactive, photolabile oligodeoxyribonucleotide probe complementary to 16S rRNA nucleotides 1397–1405 and its exploitation in identifying 30S ribosomal subunit components neighboring its target site in 16S rRNA. Nucleotides 1397–1405 lie within a single-stranded sequence that has been linked to the decoding region of *Escherichia coli* ribosomes. On photolysis in the presence of activated 30S subunits, the photolabile oligodeoxyribonucleotide probe site-specifically incorporates into proteins S1, S7, S18, and S21 (identified by SDS–PAGE, RP-HPLC, and antibody affinity chromatography) and into three separate 16S rRNA regions, specifically, nucleotides A-1396, G-1405–A-1408, and A-1492 and A-1493. These results provide clear evidence that G-1405 in 16S rRNA is within 24 Å (the distance between G-1405 and the photogenerated nitrene) of proteins S1, S7, S18, and S21 and each of the other nucleotides mentioned above, consistent with other studies of 30S internal structure. Although the probe binds to inactive 30S subunits about as well as to activated 30S subunits, photolysis of the inactive 30S·probe complex leads to a very different pattern of protein labeling, providing strong evidence, at the protein level, that the inactive to activated transition is accompanied by conformational change in the 1400 region of 16S rRNA.

The use of oligodeoxyribonucleotides (oligoDNAs) that are complementary to single-stranded rRNA sequences to study rRNA, both in its isolated form and within ribosomal subunits, has contributed to the identification of sites within rRNA that are directly linked to specific aspects of ribosomal function as well as to the placement of these sites within the subunit structure. This approach was first introduced by Bogdanov and his co-workers (Skripkin et al., 1979; Mankin et al., 1981). More recently, Hill and his co-workers (1990) have demonstrated that many single-stranded regions of rRNA can form stable complexes with their complementary oligodeoxyribonucleotides, as evidenced both by filter binding assays and by the demonstration of cleavage of rRNA at the targeted position following treatment of the complex with RNase H. By measuring the effects of added probes on specific ribosomal functions, they also obtained evidence regarding the functional importance of targeted rRNA sequences. In addition, attachment of electron microscopic markers to complementary oligoDNAs and visualization of the complexes of such oligoDNAs bound to ribosome subunits has permitted three-dimensional localization of the targeted rRNA sequence (Olson et al., 1988; Lasater et al., 1989, 1990; Oakes et al., 1990; Oakes & Lake, 1990; McWilliams & Glitz, 1991).

In recent articles (Muralikrishna & Cooperman, 1991; Cooperman et al., 1993) we have described the use of radioactive, photolabile complementary oligoDNA probes as photoaffinity labels to identify ribosomal components that neighbor functionally important single-stranded sequences of rRNA. One such sequence, comprising the highly conserved nucleotides 1397–1408 (Gutell & Woese, 1990), is of particular interest. This sequence was located within the 30S subunit at the level of the neck, near the cleft and most likely on the head of the small subunit by DNA hybridization electron microscopy (Oakes et al., 1986). There is a large body of evidence identifying it as part of the "decoding center" of the *Escherichia coli* ribosome (Zimmermann et al., 1990; Cunningham et al., 1992); it is available within 30S subunits for the binding of complementary oligoDNAs, and such binding is competitive with the poly(U)-dependent binding of $tRNA^{Phe}$ (Hill et al., 1990; Weller & Hill,1992).

In this work we convert the oligodeoxyribonucleotide 5′-CGGGCGGTG-3′ into a radioactive photoaffinity labeling reagent, *O*-(*N*-(*p*-azidobenzoyl)-6-aminohexyl)-pCGGGCGT-GA* (ABAH1405–1397A*:[1] the asterisk indicates the presence of radioactivity), and use this reagent to identify ribosomal components in the vicinity of the 16S rRNA sequence 1397–1405.

EXPERIMENTAL PROCEDURES

Materials

Buffers. The following buffers were used: TKM0.3, 40 mM Tris-HCl (pH 7.4), 60 mM KCl, and 0.3 mM $MgCl_2$; TKM10, 10 mM Tris-HCl (pH 7.4), 100 mM KCl, and 10 mM $MgCl_2$; TND, 20 mM Tris-HCl (pH 7.9), 50 mM NaCl, and 1 mM dithiothreitol.

RNase H was isolated from *E. coli* Q13 according to the method of Darlix (1975). The following materials were purchased and used without further purification: terminal deoxynucleotidyl transferase and a calibrated RNA ladder (Bethesda Research Labs), avian myeloblastosis virus reverse transcriptase (AMV-RT, Molecular Genetic Resources,

† This work was supported by NSF Grant MCB-9118072.

* Author to whom inquiries should be addressed.

® Abstract published in *Advance ACS Abstracts,* January 15, 1994.

[1] Abbreviations: ABAH, *O*-(*N*-(*p*-azidobenzoyl)-6-aminohexyl)-; AMV-RT, avian myeloblastosis virus reverse transcriptase; DMT, dimethoxytrityl; HSAB, *N*-hydroxysuccinimidyl 4-azidobenzoate; PAGE, polyacrylamide gel electrophoresis; RP-HPLC, reverse-phase high-performance liquid chromatography; SDS, sodium dodecyl sulfate; TP30, total protein from 30S subunits; nt, nucleotide(s).

0006-2960/94/0433-1392$04.50/0

Tampa, FL), *N*-hydroxysuccinimidyl 4-azidobenzoate (HSAB) and HPLC grade trifluoroacetic acid (Pierce), HPLC grade acetonitrile (Fisher), bacteriophage T4 polynucleotide kinase (New England Biolabs), chemicals used in the synthesis of oligodeoxynucleotides (Glen Research, Sterling, VA), Sep-pak C-18 cartridges (Waters), [γ-^{32}P]ATP (3000 Ci/mmol, DuPont/New England Nuclear), and [α-^{32}P]ddATP (5000 Ci/mmol, Amersham).

The 30S subunits and 16S rRNA were prepared from *E. coli* Q13 cells as described (Kerlavage & Cooperman, 1986). Activated 30S subunits were produced by incubating 30S subunits at 40 °C in TKM10 for 15 min before use. The 30S subunit concentration was calculated assuming that 1 A_{260} unit equals 78 pmol.

Synthesis and Purification of Oligodeoxyribonucleotides. cDNA 1405–1397, having the sequence 5′-CGGGCGGTG-3′, and the corresponding mismatched oligonucleotide 5′-CGGTAGGTG-3′ (MM-cDNA 1405–1397) were synthesized using procedures identical to those previously described (Muralikrishna & Cooperman, 1991). cDNA 1405–1397 ^{32}P-labeled at its 5′-end, p*1405–1397, was made by incubation of cDNA 1405–1397 with [γ-^{32}P]ATP and polynucleotide kinase and purified using Sep-pak (C-18) cartridges, according to Sambrook et al. (1989). The photolabile, radioactive cDNA, ABAH1405–1397A*, was synthesized using a procedure essentially identical to that described earlier for the synthesis of a photolabile, radioactive cDNA targeted to the 2497–2505 sequence in 23 S rRNA (Muralikrishna & Cooperman, 1991). Briefly, a hexylamine is introduced at the 5′-terminus which is coupled with HSAB, thereby introducing photolability, and the cDNA is labeled at the 3′-end using [α-^{32}P]-ddATP and terminal deoxynucleotidyl transferase (Yousaf et al., 1984).

Methods

The following methods were carried out by applying procedures to 30S subunits previously employed by us to analyze cDNA and photolabile cDNA interactions with 50S subunits (Muralikrishna & Cooperman, 1991): non-covalent binding of p*1405–1397 to 30S subunits by Millipore filtration, RNase H digestion of complexes of cDNAs either with 30S subunits or with 16S rRNA, PAGE analysis of RNase H digestion mixtures, photoincorporation of ABAH1405–1397A* into 30S subunits, determination of ABAH1405–1397A* photoincorporation into the 16S rRNA fraction of labeled 30S subunits, and localization of sites of photoincorporation into 16S rRNA by RNase H and reverse transcriptase analyses.

Proteins were prepared from ABAH1405–1397A*-labeled 30S subunits by acetic acid extraction and acetone precipitation (Kerlavage & Cooperman, 1986). Labeled proteins were identified by SDS–PAGE coupled with autoradiographic analysis (Muralikrishna & Cooperman, 1991), RP-HPLC analysis (Kerlavage et al., 1984), and agarose antibody affinity chromatography analysis (Gulle et al., 1988).

RESULTS

Non-Covalent Binding of Oligodeoxyribonucleotides. The noncovalent binding of cDNA p*1405–1397 to 30S subunits was determined using a Millipore assay (Figure 1). Binding of probe to activated 30S subunits proceeded to a plateau value of 100%, which was reached at a probe:30S subunit molar ratio of approximately 10:1. Binding of the probe to inactive subunits proceeds to approximately the same extent (Figure 1). These results are similar to those reported by Weller and Hill (1992) for the binding of cDNA oligomers

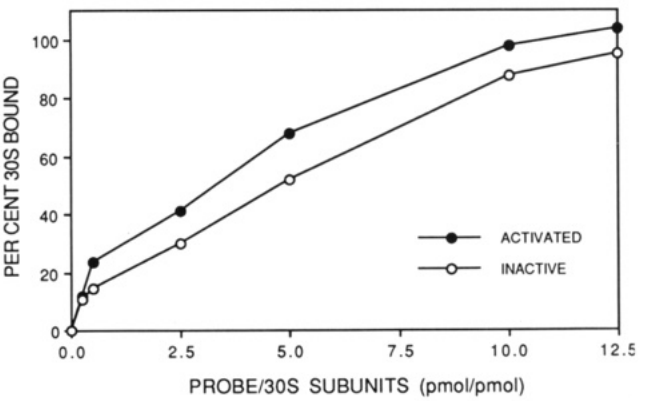

FIGURE 1: Binding of p*1405–1397 to activated and inactive 30S subunits. The 30S subunits (15 pmol) were incubated with varying amounts of p*1405–1397 (250–500 cpm/pmol) in 25 μL of TKM0.3 at 37 °C for 5 min and left on ice for 15 min, after which the $MgCl_2$ concentration was raised to 10 mM, and the incubation on ice was continued for an additional 2 h. The reaction mixtures were then diluted with 0.5 mL of cold TKM0.3 containing 10 mM $MgCl_2$ (binding buffer) and filtered through HAWP 0.45-μm nitrocellulose filters (Millipore), followed by three 1-mL washes of the filters with binding buffer. The amount of filter-bound oligonucleotide was determined by liquid scintillation counting of the dried filters.

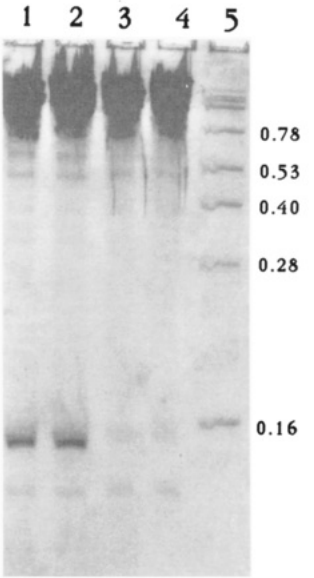

FIGURE 2: Urea–PAGE analysis of RNase H digestions. Complexes of 30S subunits (75 pmol) and 150 pmol of either cDNA 1405–1397 or ABAH1405–1397A* in a volume of 25 μL were digested with RNase H (5 units), and the phenol-extracted rRNA was analyzed. RNA bands were visualized by staining with methylene blue. Lane 1, RNase H with cDNA 1405–1397; lane 2, RNase H with ABAH1405–1397A*; lane 3, cDNA 1405–1397 without RNase H; lane 4, RNase H without added oligodeoxyribonucleotide; lane 5, RNA size markers (in kb).

1397–1403 and 1399–1406 to 30S subunits. These authors interpreted their results as indicating stoichiometric binding to the target site, an interpretation with which we have no reason to disagree.

Evidence that the binding of p*1405–1397 to 30S activated subunits occurs specifically to its complementary region in 16S rRNA is provided by the 140-nt RNA fragment that is released following RNase H treatment of the complex (Figure 2). The same fragment is obtained on RNase H digestion of the complex formed between 30S subunits and the photolabile probe ABAH1405–1397A* but is not formed in the absence of either RNase H or cDNA probe. Again in agreement with Weller and Hill (1992), by RNase H digestion we find no evidence for probe binding to rRNA at other than the target site.

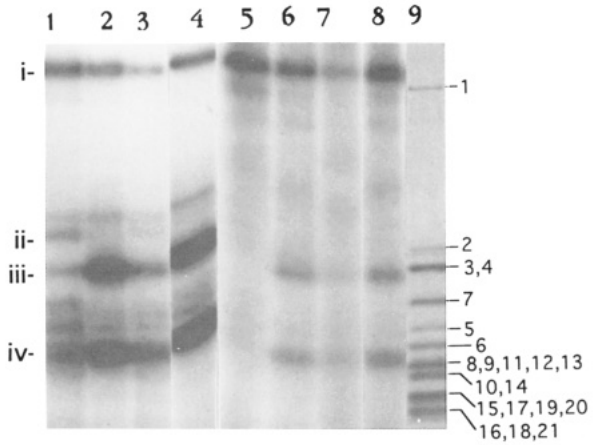

FIGURE 3: Autoradiogram of a PAGE analysis of proteins photoaffinity labeled with ABAH1405–1397A*. The reaction mixture (total volume, 75 μL), subjected to photolysis with 3000-Å lamps (Rayonet), contained 30S subunits (150 pmol) and ABAH1405–1397A* (7.5 pmol) in the absence or presence (600 pmol) of cDNA 1405–1397 or MM-cDNA 1405–1397. Lanes 1–4 display 67% acetic acid soluble fractions from 30S subunits photolyzed in the presence of ABAH1405–1397A*. Lane 1, inactive 30S subunits; lane 2, activated 30S subunits; lane 3, activated subunits in the presence of cDNA probe 1405–1397; lane 4, activated subunits in the presence of MM-cDNA 1405–1397. Lanes 5–8 are the acetic acid pellet fractions corresponding to lanes 1–4, respectively. Lane 9 displays TP30, as visualized by Coomassie Blue staining. Gels were prepared with 15% acrylamide/0.08% bis(acrylamide) in 0.75 M Tris-HCl (pH 8.8)/0.1% SDS.

Proteins S1, S7, S18, and S21 Are Specifically Labeled on Photolysis of the 30S·ABAH1405–1397A Complex.* Proteins labeled on photolysis of the 30S·ABAH1405–1397A* complex were identified by a combination of SDS–PAGE, RP-HPLC, and immunological analyses. In these experiments [30S] ≫ [ABAH1405–1397A*] in order to minimize nonspecific photoincorporation. Such photoincorporation could arise from weak binding interactions not detected by Millipore assay (see Discussion).

The results of SDS–PAGE and autoradiographic analysis of both the acetic acid soluble material (essentially all protein) and the acetic acid insoluble material (rRNA with a trace of protein) obtained from photolabeled 30S subunits are displayed in Figure 3. There are three major labeled bands, i, iii, and iv (lanes 2 and 6), and the labeling of each was reduced when photoincorporation was carried out in the presence of cDNA 1405–1397 (lanes 3 and 7). In contrast, addition of MM-cDNA 1405–1397 had no effect on photoincorporation (lanes 4 and 8).

Ribosomal protein labeled with an oligoDNA migrates in SDS–PAGE with an apparent molecular mass corresponding approximately to the sum of the protein and oligoDNA masses (Muralikrishna & Cooperman, 1991). In what follows we distinguish between actual molecular mass, calculated from a knowledge of ribosomal protein primary structure (Giri et al., 1984), and apparent molecular mass, calculated by comparison of observed band migration with a best-fit line through a plot of band migration vs the logarithm of actual molecular mass for TP30. Band i (apparent molecular mass of 66.5 kDa) clearly corresponds to labeled S1 (apparent molecular mass of 63.5 kDa; actual molecular mass of 61.2 kDa). Band iii (apparent molecular mass of 21.3 kDa) corresponds most probably to labeled S7 (apparent molecular mass of 18.4 kDa; actual molecular mass of 19.7 kDa). Labeled S5, the most likely other possibility for band iii, has an apparent molecular mass of 16 kDa and an actual molecular mass of 17.5 kDa. Assigning band iv (apparent molecular mass of 12.8 kDa) is more difficult, since proteins S15–S21

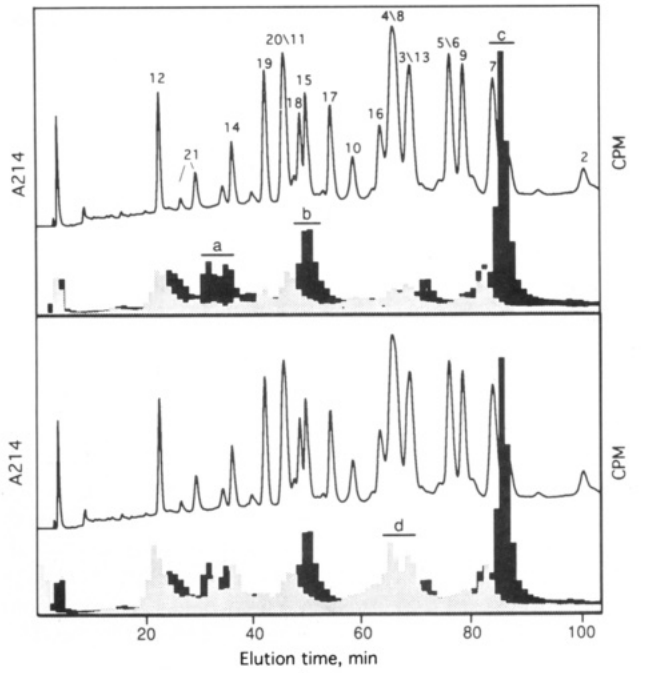

FIGURE 4: RP-HPLC analysis of TP30 from 30S subunits photolyzed with ABAH1405–1397A*. Upper panel: Activated 30S subunits (150 pmol) photolyzed with ABAH1405–1397A* (7.5 pmol) in the absence (solid bars) or presence (stippled bars) of cDNA 1405–1397 (750 pmol). Pooled peaks a–c were tested immunologically (see Figure 5). Lower panel: Solid bars, same as upper panel; stippled bars, proteins from inactivated 30S subunits photolyzed with ABAH1405–1397A* as above, in the absence of cDNA. In both panels, the trace is A_{214}, the solid bars are aligned with the trace, and the stippled bars are offset by 3 min to permit facile comparison with the solid bars. For each analysis, proteins were extracted with 67% acetic acid and precipitated with acetone. TP30 from 2 A_{260} units of photolyzed subunits was redissolved in 200 μL of 0.1% trifluoroacetic acid, applied to a SynChropak RP-P column, and eluted with the following gradient: 15–45% acetonitrile in 120 min (curve 0.2, convex gradient, Perkin-Elmer Series 4); 45–55% acetonitrile in 10 min (linear); 55–75% acetonitrile in 15 min (linear). The flow rate was 0.7 mL/min.

(actual molecular masses of 8.4–10.3 kDa) are all potential candidates.

Acetic acid extraction removes virtually all ribosomal protein from 30S subunits (Hardy et al., 1969; Jaynes et al., 1978). In earlier work (Muralikrishna & Cooperman, 1991) we observed that some cDNA-labeled protein is left behind in the rRNA pellet after acetic acid extraction, presumably because of incomplete denaturation of the heteroduplex formed between the cDNA and the rRNA. The presence of bands i, iii, and iv in lanes 6 and 8 is another illustration of this phenomenon. More labeled S1 is present in the acetic acid pellet fraction than in the acetic acid soluble fraction, reflecting the comparatively low efficiency of acetic acid extraction in the removal of S1 from 30S subunits.

Further information regarding the identity of specifically labeled proteins was provided by RP-HPLC analysis of the acetic acid extract of labeled 30S subunits (Figure 4, upper panel). Three peaks, the labeling of each of which is decreased in the presence of cDNA 1405–1397, are observed. The largest (peak c) elutes just behind S7. Of the two smaller peaks, one elutes with S15, just behind S18 (peak b), and the other, a doublet, elutes between S21 and S14 (peak a). In a separate experiment not shown, RP-HPLC analysis of band iii material extracted from a gel showed it to elute as peak c. Similar analysis of band iv material gave peaks eluting as peaks a and b.

Agarose antibody affinity chromatography analysis (Figure 5) confirms the identities of band iii/peak c material as labeled S7, of band iv/peak b material as labeled S18, and of band

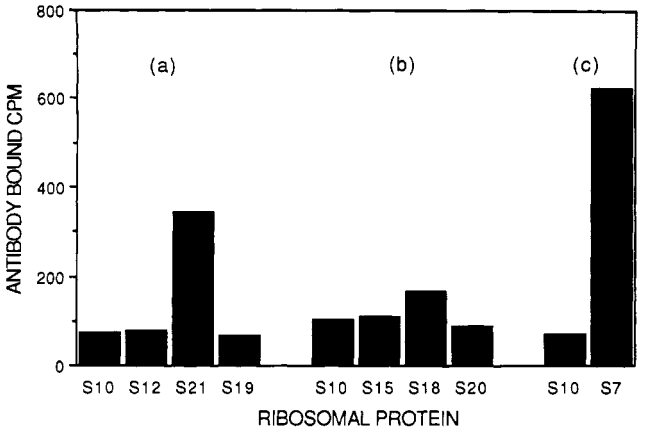

FIGURE 5: Agarose antibody affinity chromatography analysis of 30S ribosomal proteins labeled with ABAH1405–1397A*. Pooled peaks a–c from RP-HPLC separation of TP30 derived from 30S subunits photolyzed with ABAH1405–1397A* in the absence of added cDNA (Figure 4, upper panel) were analyzed separately. Antibody to protein S10 was used as a negative control. Bars denote counts per minute bound to antibody to each of the indicated ribosomal proteins, performed as described by Gulle et al. (1988).

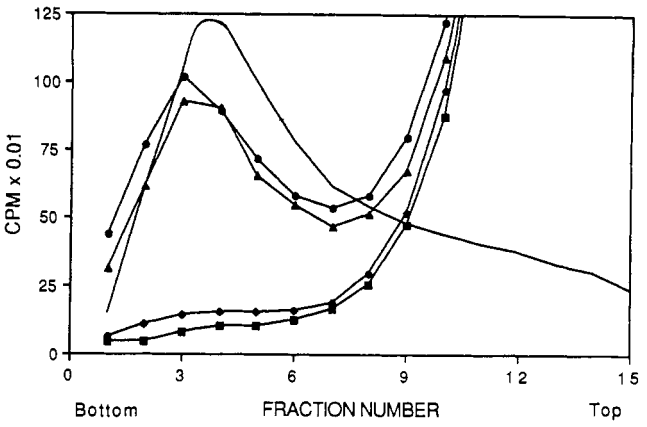

FIGURE 6: Photoincorporation of ABAH1405–1397A* into 16S rRNA. The 30S subunits (150 pmol) were incubated with ABAH1405–1397A* (50 pmol) in a total volume of 75 μL: (■) without photolysis; (●) with photolysis; (◆) with photolysis in the presence of cDNA 1405–1397 (750 pmol); (▲) with photolysis in the presence of MM-cDNA 1405–1397 (750 pmol). All samples were analyzed by sucrose gradient centrifugation in the presence of urea and SDS (Muralikrishna & Cooperman, 1991). The solid line without symbols is a trace of the absorbance at 260 nm. Photoincorporation levels were as follows: with photolysis, 9.5 pmol; with photolysis in the presence of cDNA 1405–1397, 1.1 pmol; with photolysis in the presence of MM-cDNA 1405–1397, 7 pmol; without photolysis, 0.3 pmol.

iv/peak a material as labeled S21. It would thus appear that photoincorporation of an oligonucleotide has the effect of slightly retarding elution of ribosomal protein from a reverse-phase column and that, not unexpectedly, such retardation is more marked for smaller proteins. Identification of the peak a doublet with labeled S21 is consistent with the observation in this laboratory that S21 often elutes as a doublet on RP-HPLC analysis.

Photoincorporation of ABAH1405–1397A* proceeds to a lower extent into inactive than into activated 30S subunits. The most noteworthy differences in the pattern of protein labeling are the appearance of a new band, ii, on SDS–PAGE analysis not seen with active subunits (Figure 3, lane 1); the large reduction in S7 and S18 labeling on RP-HPLC analysis (Figure 4, lower panel); and the appearance of a new, doublet radioactivity peak, d, on RP-HPLC analysis. Band ii (apparent molecular mass of 28.2 kDa) corresponds to labeled S3 and/or S4 (comigrating with an apparent molecular mass of 24.5 kDa; actual molecular masses of 25.9 and 23.1 kDa, respectively). Identification of S3 and S4 as the major proteins labeled to a greater extent in inactive vs activated 30S subunits is also consistent with the elution position of peak d in Figure 4 (lower panel), since one part of the doublet is slightly retarded with respect to S4/S8, while the other is slightly retarded with respect to S3/S13.

Photoincorporation of ABAH1405–1397A into 16S rRNA.* Activated 30S subunits, labeled with ABAH1405–1397A* under conditions maximizing site-specific labeling ([30S] ≫ [ABAH1405–1397A*]), were subjected to sucrose gradient centrifugation in an SDS–urea buffer, conditions that remove both protein and non-covalently bound cDNA probe (Muralikrishna & Cooperman, 1991). The results presented in Figure 6 show that incorporation of ABAH1405–1397A* into 16S rRNA is light-dependent, is almost completely abolished on addition of cDNA 1405–1397, and is little affected by the addition of MM-cDNA 1405–1397.

Partial Localization of ABAH1405–1397A Photoincorporation Sites in 16S rRNA.* As in our earlier work (Muralikrishna & Cooperman, 1991), partial localization of oligoDNA photoincorporation into rRNA was carried out by PAGE and autoradiographic analysis of the products of RNase H treatment (Figure 7). The apparent sizes of labeled fragments (as estimated from a semilog plot of the number of nucleotides vs migration distance for a set of DNA size markers, lane 1) are typically larger (10–20 nt) than would be expected for the corresponding unlabeled fragments generated with complete RNase H digestion. This is due to both the size of the photoincorporated probe itself (10 nt) and the "frayed" ends that sometimes result from incomplete RNase H digestion.

Autoradiographic analysis of a PAGE separation of the reaction mixture resulting from RNase H digestion of ABAH1405–1397A*-labeled 16S rRNA, taken up in a non-denaturing buffer, reveals the presence of a ^{32}P-labeled 160-nt fragment (lane 3). This result indicates that the specific heteroduplex between photolyzed, covalently incorporated ABAH1405–1397A* and 16S rRNA is re-formed under the conditions used for RNase H digestion, providing a site for RNase H cleavage. It also shows that photoincorporation into 16S rRNA takes place between nucleotides 1397/1405 and 1542.

Similar analyses were performed on ABAH1405–1397A*-labeled 16S rRNA that had been hybridized with cDNA probes added one at a time (1367–1358, 1461–1445, and 1504–1495; Figure 7, lanes 4, 5, and 6, respectively). The results presented in lane 5, showing two fragment clusters, one centered at about 95 nt and another centered at about 55 nt, provide clear evidence for two sites of photoincorporation between nucleotides 1397/1405 and 1542, one between nucleotides 1445/1461 and 1542, and one between nucleotides 1397/1405 and 1445/1461. The appearance of a single dark cluster centered at 110 nt on RNase H digestion in the presence of cDNA 1504–1495 (lane 6) indicates that both of these sites fall between nucleotides 1397/1405 and 1495/1504.

Analyses were also performed following addition of 16S rRNA cDNA probes 268–259, 526–518, 795–787, 920–909, and 1339–1330 to ABAH1405–1397A*-labeled 16S rRNA, either one at a time or in pairs, in an effort to determine whether there were other major sites of photoincorporation between 16S rRNA nucleotides 1 and 1397; no such sites were found.

Identification of Specific Nucleotides in 16S rRNA into Which ABAH1405–1397A Photoincorporates.* Specific sites of photoincorporation within the two nucleotide regions

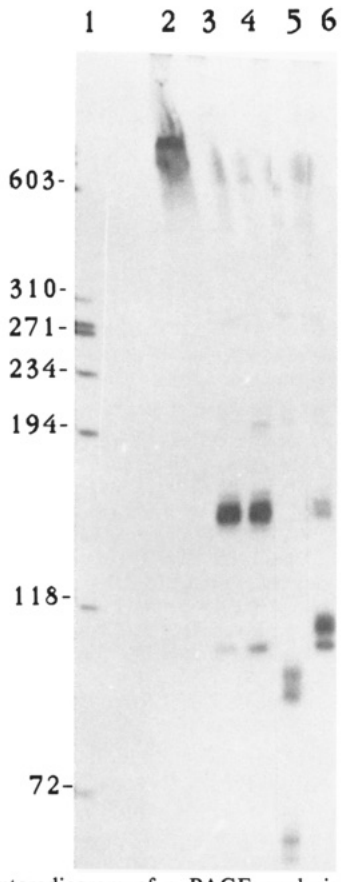

FIGURE 7: Autoradiogram of a PAGE analysis of 16S rRNA photoaffinity labeled with ABAH1405–1397A* and treated with cDNA probes and RNase H. In a typical experiment, labeled rRNA (16 pmol), purified by sucrose gradient centrifugation in the presence of urea and SDS (Figure 6), was incubated with an equimolar amount of cDNA in 10 μL of TND buffer and digested with RNase H. Lane 1, DNA size markers (in kb); lane 2, labeled 16S rRNA in the absence of added RNase H; lane 3, labeled 16S rRNA digested with RNase H; lane 4, labeled 16S rRNA hybridized with cDNA probe 1367–1358 and digested with RNase H; lane 5, labeled 16S rRNA hybridized with cDNA probe 1461–1445 and digested with RNase H; lane 6, labeled 16S rRNA hybridized with cDNA probe 1504–1495 and digested with RNase H.

described above were identified using the primer extension approach (Muralikrishna & Cooperman, 1991) on 16S rRNA extracted from 30S subunits photolabeled in the presence of ABAH1405–1397. Both ABAH1405–1397-photolabeled 16S rRNA and control 16S rRNA prepared from 30S subunits photolyzed in the absence of probe were hybridized to single-stranded oligodeoxynucleotide primers complementary to 16S rRNA, and the resulting heteroduplexes were examined as substrates for AMV-RT by PAGE and autoradiographic analysis.

The results of such analyses are shown in Figure 8. Panel A shows clear pauses or stops in analysis of the photoincorporation experiment (lane 3), not seen in the analysis of the controls (lanes 1 and 2), at positions U-1406–C-1409 and C-1397, implicating nucleotides G-1405, U-1406, m^5C-1407, A-1408, and A-1396 as sites of photoincorporation. Similarly, panel B of Figure 8 shows pauses or stops at A-1493 and G-1494, implicating A-1492 and A-1493 as sites of photoincorporation. Thus ABAH1405–1397 photoincorporates not only into the rRNA single-stranded region to which it is complementary but into one other region as well, separated by more than 80 nt within the 16S rRNA primary structure.

DISCUSSION

Our results indicate that, within activated 30S subunits, proteins S1, S7, S18, and S21 and nucleotides 1396, 1405–1408, 1492, and 1493 are each labeled by the photolabile oligonucleotide ABAH1405–1397A* specifically bound to its complementary sequence in 16S rRNA, and provide strong evidence for a conformational change accompanying the conversion of inactive 30S subunits to the activated form.

Evidence that photoincorporation into proteins S1, S7, S18, and S21 proceeds site-specifically from the 1397–1405 target site comes from the results presented in Figures 3 and 4. Thus, addition of cDNA1405–1397 reduces photoincorporation into these proteins, as would be expected from competitive binding to a common site. In contrast, the labeling of some proteins is little affected by the addition of cDNA1405–1397, an indication that such proteins are not labeled site-specifically. The experiments employing MM-cDNA 1405–1397 were carried out to test whether the specific site from which labeling occurs is, in fact, the target site. We reasoned that, with two mismatches in the middle of its sequence, MM-cDNA 1405–1397 would compete only very poorly with ABAH1405–1397A* binding to the target sequence but, with seven of the nine other residues conserved, could compete with the binding of ABAH1405–1397A* to other sites in the 30S subunit, if such binding occurred. Thus, the lack of effect of MM-cDNA 1405–1397 on the photoincorporation of ABAH1405–1397A* into proteins S1, S7, S18, and S21 indicates that these proteins are labeled from the target site.

By the same criteria, the results presented in Figure 6 demonstrate that essentially all photoincorporation of ABAH1405–1397A* into rRNA arises from ABAH1405–1397A* specifically bound to the complementary sequence in 16S rRNA. That is, there is a large decrease in photoincorporation for photolyses carried out in the presence of cDNA 1405–1397, but addition of MM-cDNA 1405-1397 has little effect. The lack of nonspecific labeling of 16S rRNA contrasts with the appreciable nonspecific labeling found for 30S protein (Figure 4, upper panel). We assume that the latter arises either from reactions with nitrene generated in solution or from photolyzed ABAH1405–1397A* bound to weak sites on the surface of the 30S subunit. Such reactions are less likely to occur with 16S rRNA, since most of it is buried within the 30S structure.

Assuming that labeling proceeds from the photogenerated nitrene, a part of each of the ribosomal components we identify as being site-specifically labeled in activated 30S subunits lies within 24 Å of G-1405. These ribosomal components can thus be considered as constituting at least part of the neighborhood of G-1405, a conclusion which is fully consistent with results obtained by others in related studies and which strengthens current models describing the immediate environment of 16S nucleotides 1397–1405 (Cunningham et al., 1992; Dontsova et al., 1992a,b; Brimacombe et al., 1993). Evidence for the mutual proximity of the four specifically labeled proteins comes from several sources. First, cross-linking studies on 30S subunits have demonstrated that each of the proteins S1 (Kenner, 1973; Czernilofsky et al., 1975), S7 (Greuer et al., 1987), and S21 (Kyriatsoulias et al., 1986; Osswald et al., 1987) can be cross-linked to the 3′-terminus of 16S rRNA and that S18 can be cross-linked to both S21 and S1 (Lambert et al., 1983). Second, neutron diffraction studies demonstrate the close proximity of the centers of mass of S18 and S21 (Capel et al., 1988). Third, immunoelectron microscopy places S7, S18, and S21 along the cleft between the head and platform regions of the 30S subunit, with S18 and S21 close together in the platform and S7 lying across the cleft in the head region (Stöffler-Meilicke & Stöffler, 1990; Scheinman et al., 1992). Fourth, and most pertinent for our work, Dontsova et al. (1991) and Stade et al. (1989) have

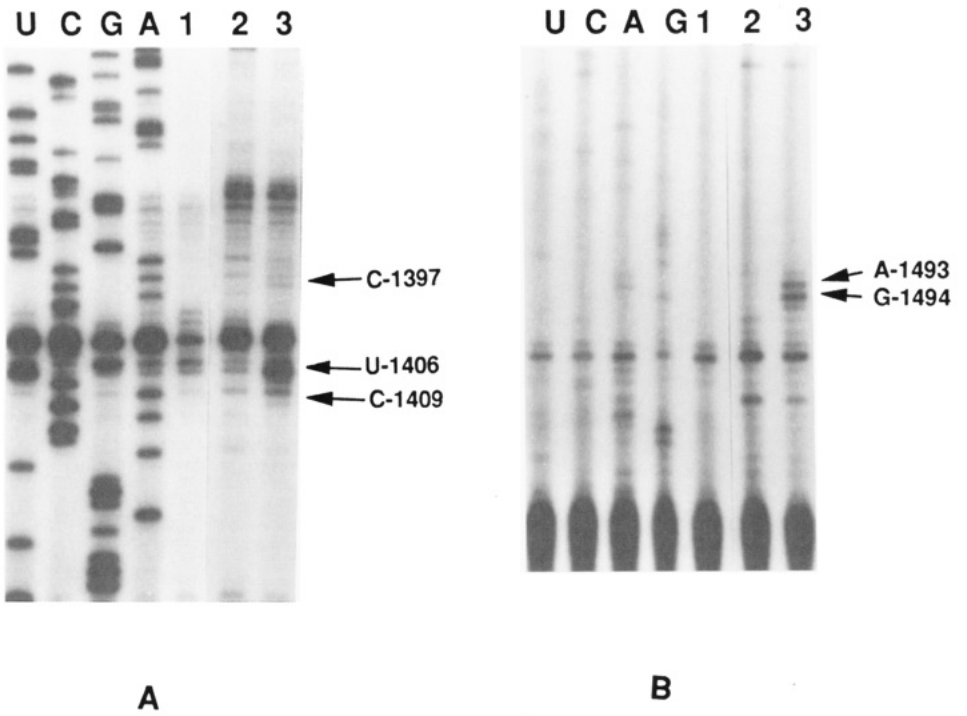

FIGURE 8: Autoradiograms showing reverse transcription of RNA photolabeled with ABAH1405–1397. Photoincorporation was carried out in a reaction mixture containing 150 pmol of 30S subunits and 750 pmol of ABAH1405–1397 in a total volume of 75 μL. Lane 1, primer extension on rRNA extracted from 30S subunits incubated with ABAH1405–1397 without photolysis; lane 2, primer extension on rRNA extracted from 30S subunits photolyzed in the absence of ABAH1405–1397; lane 3, primer extension on rRNA extracted from 30S subunits photolyzed in the presence of ABAH1405–1397. Lanes U, C, G, and A are sequencing lanes generated in the presence of ddATP, ddGTP, ddCTP, and ddTTP, respectively. Nucleotides at which pauses or stops are observed are indicated. Primers used are 1461–1445 in panel A and 1542–1527 in panel B.

demonstrated photoinduced cross-links between synthetic mRNAs, 30–35 nt long, containing 4-thiouridine in place of uridine at several sites, and the same four proteins, S1, S7, S18 and S21, labeled site-specifically in this work. These latter papers report cross-links to proteins S7, S18, and S21 from a 7-nt stretch (designated –4 to +3, where +1 to +3 correspond to the AUG initiation codon) within the mRNA. It is also pertinent that proteins S3 and S4, which we find as major sites of labeling in inactive rather than activated 30S subunits (Figure 4, lower panel), are also found as minor labeling sites by Dontsova et al. (1991) and that either S3 or S3 and S4 have been found as major sites of mRNA affinity labeling in several other studies [as reviewed in Cooperman (1987); more recent examples may be found in Vladimirov et al. (1990), Dontsova et al. (1992b), and Rinke-Appel et al. (1991)].

The proximity we find between nucleotides 1405, 1492, and 1493 is fully consistent with the long accepted secondary structure model for 16S rRNA that posits base pairing between nucleotides 1409–1412 and 1491–1488 (Noller, 1984), as well as with more recent evidence, based on comparative sequence analysis (Gutell & Woese, 1990) and site-specific mutagenesis studies [summarized in Cunningham et al. (1992, 1993)], for the functional importance of the following additional base pairs between these two regions of 16S rRNA: 1399–1504, 1401–1501, 1404–1497, 1405–1496, and 1407–1494. In addition, Döring et al. (1992) have demonstrated direct UV-induced cross-links between nucleotides 1402/1405 and 1498/1504. Evidence for a further proximity of the 1400 region to the 3′-terminus of 16S rRNA comes from the 4-thiouridine-containing mRNA work already mentioned, in which it has been demonstrated that position –4 cross-links to the 3′-end of 16S rRNA (Dontsova et al., 1991) and position +4 cross-links to 16S rRNA 1402/1407 (Rinke-Appel et al., 1993). The proximity of the 1400 region to the 1500 and 3′-terminal regions is consistent with results obtained by both DNA hybridization electron microscopy and immunoelectron microscopy (Glitz & Politz, 1977; Olson et al., 1988; Lasater et al., 1989; Oakes et al., 1990).

There is now good evidence for at least two conformational changes in the 30S subunit centered about the 1400 region. One is the change expected to result from the conversion of the 30S conformer having base pairing between nucleotides in the 1400 and 1500 regions, which is apparently necessary for some aspects of ribosomal function (Cunningham et al., 1992), to a conformer in which the 1400 region readily forms a heteroduplex with the 1397–1405 cDNA probe coming from solution. The second is the inactive to activated transition that results from brief heating of isolated 30S subunits at 40 °C in the presence of 10 mM Mg^{2+} (Zamir et al., 1971). As first demonstrated by Weller and Hill (1992) and confirmed in the present work (Figure 1), this transition has little effect on the availability of the 1400 region to a cDNA probe. However, the inactive to activated 30S transition is accompanied by large changes in the chemical reactivity of nucleotides within 16S rRNA, with the great majority of those changes occurring in the 1400, 1500, and 3′-terminal regions of rRNA (Moazed et al., 1986). The present work, showing that 30S activation is accompanied by large increases in S18 and especially S7 labeling and a decrease in S3 and S4 labeling (Figure 4, lower panel), provides another indication, this time at the protein level, of a conformational change in the 1400 region during the inactive to activated transition.

Our current results, together with the prior results cited above, provide strong evidence for a neighborhood in activated 30S subunits in which the 1500 and 3′-terminal regions of rRNA and proteins S1, S7, S18, and S21 are each in close proximity to the 1400 region, a neighborhood functionally important as the decoding center of the ribosome (Zimmermann et al., 1990; Cunningham et al., 1992). More speculatively, our results suggest that the inactive to activated transition in 30S subunits results in a conformational change

moving the 1400 region away from S3 and S4 and toward S7 and S18. Finally, our results provide an example of the effectiveness of photolabile derivatives of oligodeoxyribonucleotides, complementary to rRNA, in identifying neighboring components of single-stranded rRNA within different conformational states of ribosomal subunits.

ACKNOWLEDGMENT

We are grateful to Dr. Richard Brimacombe for conducting the agarose antibody affinity chromatography analyses of labeled 30S proteins, to Dr. Michael Mitchell of the University of Pennsylvania Cancer Center DNA facility for the synthesis of DNA oligomers, and to Ms. Nora Zuño for excellent technical assistance.

REFERENCES

Brimacombe, R., Döring, T., Greuer, B., Jünke, N., Mitchell, P., Müller, F., Osswald, M., Rinke-Appel, J., & Stade, K. (1993) in *The Translational Apparatus* (Nierhaus, K. H., Subramanian, A. R., Erdmann, V. A., Franceschi, F., & Wittmann-Liebold, B., Eds.) pp 433–444, Plenum Publishing, New York.

Capel, M., Kjeldgaard, M., Engelman, D., & Moore, P. (1988) *J. Mol. Biol. 200*, 65–87.

Cooperman, B. S. (1987) *Pharmacol. Ther. 34*, 271–302.

Cooperman, B. S., Muralikrishna, P., & Alexander, R. (1994) in *The Translational Apparatus* (Nierhaus, K. H., Subramanian, A. R., Erdmann, V. A., Franceschi, F., & Wittmann-Liebold, B., Eds.) pp 465–476, Plenum Publishing, New York.

Cunningham, P., Nurse, K., Bakin, A., Weitzmann, C., Pflumm, M., & Ofengand, J. (1992) *Biochemistry 31*, 12012–12022.

Cunningham, P., Nurse, K., Weitzmann, C., & Ofengand, J. (1993) *Biochemistry 32*, 7172–7180.

Czernilofsky, A. P., Kurland, C. G., & Stöffler, G. (1975) *FEBS Lett. 58*, 281–284.

Darlix, J. L. (1975) *Eur. J. Biochem. 51*, 369–376.

Dontsova, O., Kopylov, A., & Brimacombe, R. (1991) *EMBO J. 10*, 2613–2620.

Dontsova, O., Dokudovskaya, S., Kopylov, A., Bogdanov, A., Rinke-Appel, J., Jünke, N., & Brimacombe, R. (1992a) *EMBO J. 11*, 3105–3116.

Dontsova, O., Rosen, K., Skrjabin, G., Bogdanova, S., Skripkin, E., Kopylov, A., & Bogdanov, A. (1992b) *Biochimie 74*, 363–371.

Döring, T., Greuer, B., & Brimacombe, R. (1992) *Nucleic Acids Res. 20*, 1593–1597.

Giri, L., Hill, W. E., Wittmann, H. G., & Wittmann-Liebold, B. (1984) *Adv. Prot. Chem. 36*, 1–78.

Glitz, D. G., & Politz, S. (1977) *Proc. Natl. Acad. Sci. U.S.A. 74*, 1468–1472.

Greuer, B., Osswald, M., Brimacombe, R., & Stöffler, G. (1987) *Nucleic Acids Res. 15*, 3241–3255.

Gulle, H., Hoppe, E., Osswald, M., Greuer, B., Brimacombe, R., & Stöffler, G. (1988) *Nucleic Acids Res. 16*, 815–832.

Gutell, R., & Woese, C. R. (1990) *Proc. Natl. Acad. Sci. U.S.A. 87*, 663–667.

Hardy, S. J. S., Kurland, C. G., Voynow, P., & Mora, G. (1969) *Biochemistry 8*, 2897–2905.

Hill, W. E., Weller, J., Gluick, T., Merryman, C., Marconi, R. T., Tassanakajohn, A., & Tapprich, W. E. (1990) in *The Ribosome: Structure, Function, & Evolution* (Hill, W. E., Dahlberg, A., Garrett, R. A., Moore, P. B., Schlesinger, D., & Warner, J. R., Eds.) pp 93–106, American Society of Microbiology, Washington, DC.

Jaynes, E. N., Jr., Grant, P. G., Giangrande, G., Wieder, R., & Cooperman, B. S. (1978) *Biochemistry 17*, 561–569.

Kenner, R. A. (1973) *Biochem. Biophys. Res. Commun. 51*, 932–938.

Kerlavage, A. R., & Cooperman, B. S. (1986) *Bichemistry 25*, 8002–8010.

Kerlavage, A. R., Weitzmann, C. J., & Cooperman, B. S. (1984) *J. Chromatogr. 317*, 201–212.

Kyriatsoulis, A., Maly, P., Greuer, B., Brimacombe, R., Stöffler, G., Frank, R., & Blöcker, H. (1987) *Nucleic Acids Res. 14*, 1171–1187.

Lambert, J. M., Boileau, G., Cover, J. A., & Traut, R. R. (1983) *Biochemistry 22*, 3913–3920.

Lasater, L. S., Cann, P. A., & Glitz, D. G. (1989) *J. Biol. Chem. 264*, 21798–21805.

Lasater, L. S., Montesano-Roditis, L., Cann, P. A., & Glitz, D. G. (1990) *Nucleic Acids Res. 18*, 477–485.

Mankin, A. S., Skripkin, E. A., Chichkova, N. V., Kopylov, A. M., & Bogdanov, A. A. (1981) *FEBS Lett. 131*, 253–256.

McWilliams, R. A., & Glitz, D. G. (1991) *Biochimie 73*, 911–918.

Moazed, D., Van Stolk, B., Douthwaite, S., & Noller, H. (1986) *J. Mol. Biol. 191*, 483–493.

Muralikrishna, P., & Cooperman, B. S. (1991) *Biochemistry 30*, 5421–5428.

Noller, H. (1984) *Annu. Rev. Biochem. 53*, 119–162.

Oakes, M. I., & Lake, J. A. (1990) *J. Mol. Biol. 211*, 907–918.

Oakes, M., Clark, M., Henderson, E., & Lake, J. A. (1986) *Proc. Natl. Acad. Sci. U.S.A. 83*, 275–279.

Oakes, M., Scheinman, A., Atha, T., Shankweiler, G., & Lake, J. A. (1990) in *The Ribosome: Structure, Function, & Evolution* (Hill, W. E., Dahlberg, A., Garrett, R. A., Moore, P. B., Schlesinger, D., & Warner, J. R., Eds.) pp 180–193, American Society of Microbiology, Washington, DC.

Olson, H. M., Lasater, L. S., Cann, P. A., & Glitz, D. G. (1988) *J. Biol. Chem. 263*, 15196–15204.

Osswald, M., Greuer, B., Brimacombe, R., Stöffler, G., Bäumert, H., & Fasold, H. (1987) *Nucleic Acids Res. 15*, 3221–3240.

Rinke-Appel, J., Jünke, N., Stade, K., & Brimacombe, R. (1991) *EMBO J. 10*, 2195–2202.

Rinke-Appel, J., Jünke, N., Brimacombe, R., Dokudovskaya, S., Dontsova, O., & Bogdanov, A. (1993) *Nucleic Acids Res. 21*, 2853–2859.

Sambrook, J., Maniatis, T., & Fritsch, E. F. (1989) in *Molecular Cloning: A Laboratory Manual*, 2nd ed., pp 11–39, Cold Spring Harbor Laboratory Press, Cold Spring Harbor, NY.

Scheinman, A., Atha, T., Aguinaldo, A., Kahan, L., Shankweiler, G., & Lake, J. A. (1992) *Biochimie 74*, 307–317.

Skripkin, E. A., Kopylov, A. M., Bogdanov, A. A., Vinogradov, S. V., & Berlin, Yu. A. (1979) *Mol. Biol. Rep. 5*, 221–224.

Stade, K., Rinke-Appel, J., & Brimacombe, R. (1989) *Nucleic Acids Res. 17*, 9889–9908.

Stöffler-Meilicke, M., & Stöffler, G. (1990) in *The Ribosome: Structure, Function, & Evolution* (Hill, W. E., Dahlberg, A., Garrett, R. A., Moore, P. B., Schlesinger, D., & Warner, J. R., Eds.) pp 123–133, American Society of Microbiology, Washington, DC.

Vladimirov, S., Babkina, G., Venijaminova, A., Gimautdinova, O., Zenkova, M., & Karpova, G. (1990) *Biochim. Biophys. Acta 1048*, 245–256.

Weller, J., & Hill, W. (1992) *Biochemistry 31*, 2748–2757.

Yousaf, S. I., Carroll, A. R., & Clarke, B. E. (1984) *Gene 27*, 309–313.

Zamir, A., Miskin, R., & Elson, D. (1971) *J. Mol. Biol. 60*, 347–364.

Zimmerman, R., Thomas, C. R., & Wower, J. (1990) in *The Ribosome: Structure, Function, & Evolution* (Hill, W. E., Dahlberg, A., Garrett, R. A., Moore, P. B., Schlesinger, D., & Warner, J. R., Eds.) pp 331–347, American Society of Microbiology, Washington, DC.